Horizontal Coherence of Temperature Microstructure[1]

J. A. ELLIOTT AND N. S. OAKEY

Bedford Institute of Oceanography, Dartmouth, Nova Scotia, Canada

(Manuscript received 29 August 1974, in revised form 4 March 1975)

ABSTRACT

Temperature gradient records from vertical lowerings of an array of four thermometers are used to trace microstructure features horizontally over a distance of 46 cm. Identifiable features are found to have a slope and a vertical velocity or curvature with a statistical distribution similar to that expected from an internal wave field superimposed on horizontally-layered microstructure. The horizontal extent of microstructure with a vertical scale greater than 5 cm is at least an order of magnitude greater than its vertical scale.

1. Introduction

The three-dimensional structure of small-scale temperature gradients has been investigated with an array of four thermometers at a site in Denmark Strait during September 1973. Our studies were designed to obtain simultaneous vertical profiles of temperature microstructure over a horizontal scale of about half a meter and to determine whether the loss of coherence in the horizontal could be a result of internal wave distortion as well as the tendency toward such features becoming isotropic.

The spectra of vertical temperature gradient for profiles obtained in the Denmark Strait are similar to those described by Gregg *et al.* (1973) for data from the San Diego Trough. They consider their spectra to consist of three ranges, each with a source identifiable from the vertical temperature profile. Wavelengths greater than 100 m can be related to the mean gradient; shorter wavelengths down to about a meter correspond to intermediate-scale irregularities; and most of the variance at wavelengths less than a meter is related to features called microstructure. The same divisions apply to our Denmark Strait data where irregularities in the vertical profile with a vertical scale $\gtrsim 1$ m arise from relatively permanent features that appear to be advective in origin. Those with a vertical scale of less than a meter are highly variable in space and time and will be referred to as microstructure. In Fig. 1, two representative spectra are compared with the schematic spectrum of Gregg *et al.* (their Fig. 9).

Many studies have traced dominant features or layers over horizontal distances of a kilometer or more. Stommel and Federov (1967), for example, found "laminae" greater than 2 m thick that extended horizontally at least 2 km, while Osborn and Cox (1972) traced the dominant "high gradient" temperature features of thickness typically greater than a meter over distances of 750 m or more. In most cases these dominant features will contribute to the temperature gradient spectrum at intermediate scales and appear to be linked with or were formed in association with horizontal advection.

Embedded within the intermediate-scale layers are microstructure gradients. As part of an earlier study in the vicinity of the Gulf Stream we attempted to trace these small-scale features in the horizontal with a two-point array having a 42 cm horizontal separation. This initial measurement showed no significant coherence for structures with a vertical wavelength $\lesssim 0.5$ m. The low horizontal coherence was interpreted to result in part from the structures being tilted at a variety of angles and being distorted by the convergences and divergences of short-wavelength internal waves. A similar interpretation of the tilting of the gradients by short-wavelength, large-amplitude internal waves was used by Hacker (1973) to explain the variation in time for an identifiable gradient to arrive at two horizontally spaced probes on lowerings in the region of the San Diego Trough.

There is presently widespread interest in the relation between microstructure and internal waves. One school of thought attributes the formation of microstructure, other than the double-diffusive type, to shear instability made critical by the interaction of internal waves (Garrett and Munk, 1972). With this concept of shear instability and the associated short-wavelength, high-amplitude internal waves, similar to those described by Woods (1968), it is reasonable to expect microstructure to be linked to internal wave motion in the water column.

Our study of the three-dimensional character of microstructure with vertical scales of 1 m to 1 cm was

[1] Contribution of the Bedford Institute of Oceanography.

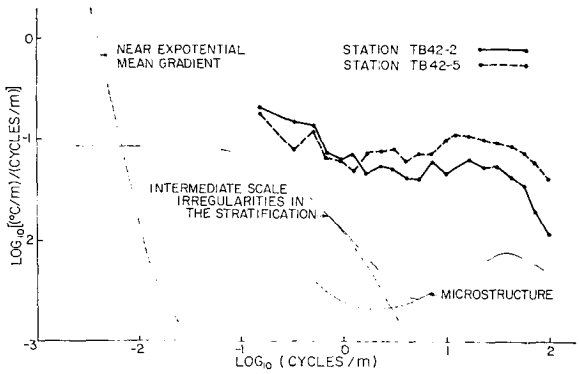

FIG. 1. Spectra of temperature microstructure from the Denmark Strait site. Also shown is the schematic intermediate and microstructure spectrum of Gregg *et al.* (1973).

part of a general survey of microstructure in the Denmark Strait and was carried out from the CSS *Hudson* while she participated in the OVERFLOW '73 expedition. The data were obtained by attaching an array of thin-film thermometers to a vertical profiler called OCTUPROBE.

2. Experimental array—OCTUPROBE

Our microstructure measurements have been obtained using our standard instrument package called OCTUPROBE (Oceanic Turbulence Probe). It consists of a 1.5 m long pressure housing to contain electronic circuitry and is surrounded by an open protective framework. The package contains a conventional salinity-temperature-depth (STD) recorder, a three-axis accelerometer, and the facility to incorporate a wide variety of microstructure sensors. These probes are rigidly attached to the pressure housing on "stings" to project them ahead of the instrument wake. The package is attached to the ship by a multiconductor cable which is used to supply power and return data signals through standard FM-FM telemetry techniques.

Most ship motion is decoupled from the OCTUPROBE by using a tethered-terminal velocity configuration. Glass floats attached 3 m above the instrument were adjusted to produce the necessary drag and buoyancy for a free-fall terminal velocity of about 1 m s^{-1}. During descent cable is paid out at a rate sufficient to keep it slack. The heavy pressure case and buoyant spheres provide a stable unit, vertically aligned.

Instrument motion is monitored with accelerometers and a pressure sensor. Fig. 2 illustrates the main features of the fluctuating instrument motion. The mean vertical velocity $\bar{V}$, as determined from the pressure sensor, slowly varies by about 10% during a fall of 1 km. Under severe conditions, ship motion causes fluctuations in the vertical velocity. Such high-frequency fluctuations (>0.1 Hz) are monitored by a vertical accelerometer; its signal (Fig. 2) is integrated to determine the instantaneous velocity, $V-\bar{V}$. The tilt of the instrument is measured by two mutually perpendicular and horizontal accelerometers. A typical record, as shown in Fig. 2, indicates maximum tilts of 3° occurring at surface wave frequencies.

The thermometer array is a special arrangement of probes mounted on the leading end of OCTUPROBE. Four thermometers are arranged at the corners of an inverted pyramid (Fig. 3). Three of the thermometers (T_2,T_3,T_4) are positioned at the corners of a horizontal equilateral triangle, 46 cm on the side. The fourth thermometer (T_1) is placed ahead of the other three by a distance D adjustable up to 1 m. During measurements, T_1 passes through a point approximately midway between T_2 and T_4. Each thermometer is positioned out of the wake of any part of OCTUPROBE. The three sensors in the horizontal plane are used to describe horizontal continuity and tilt of a feature. T_1 gives information about short-term time changes.

The sensing elements of the thermometers are conical, thin-film probes with quartz coating. These high-frequency response sensors form one arm of an ac temperature bridge. To maintain accuracy all signals are compared at low frequency to the STD temperature. To cover the desired dynamic range, the time derivative of the temperature signal, obtained using an electronic differentiator with a high-frequency cutoff of 100 Hz, is also recorded. By use of the mean vertical velocity, the time derivative can be converted to a depth derivative. The noise level of the system permits monitoring of the temperature gradient down to about 5×10^{-2} °C m^{-1}.

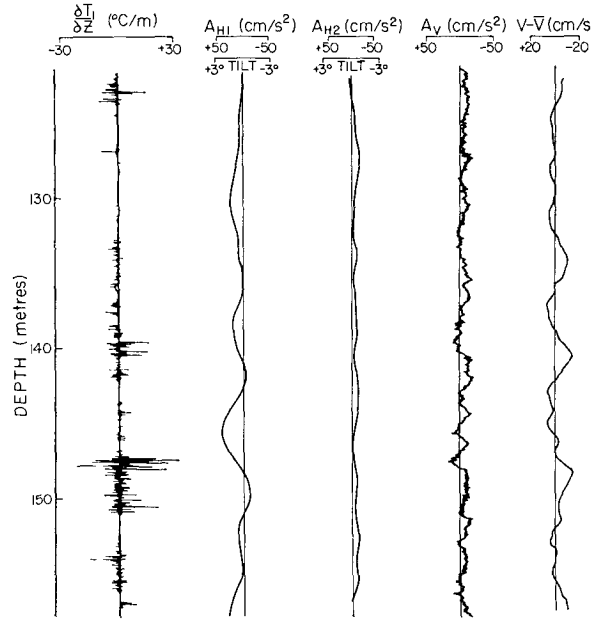

FIG. 2. OCTUPROBE motion illustrated by the record of accelerometers A_{H1}, A_{H2} and A_V, and instantaneous velocity $V-\bar{V}$ (the integral of A_V) for a 35 m length of record.

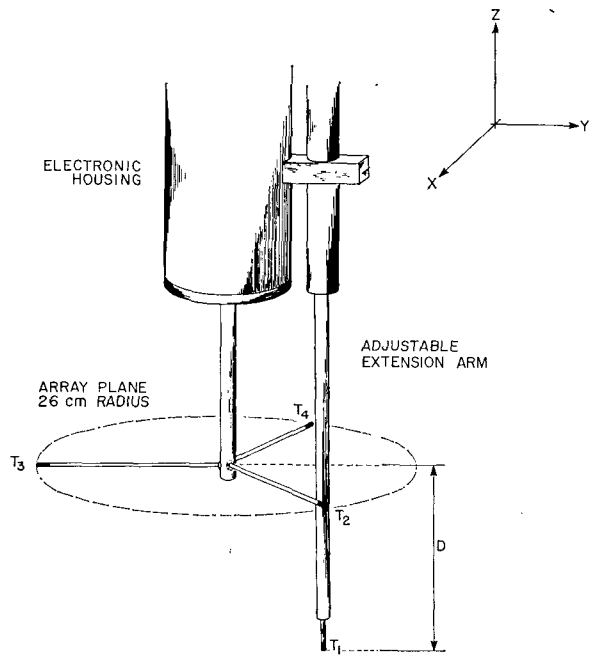

FIG. 3. OCTUPROBE with thermometer array attached.

The frequency response of all probes was tested in a tow tank by the method outlined by Fabula (1962). For velocities near the lowering speed of OCTUPROBE, between 0.8 and 1 m s^{-1}, T_2, T_3 and T_4 have a time response $\tau \approx 0.008$ s, while T_1 has a $\tau \approx 0.005$ s. The forward thermometer has a slightly better response to small-scale features than the other three.

Spectrum and cross-spectrum statistics were calculated digitally using a sampling period of 3 ms (approximately 3 samples per centimeter) and employing fast Fourier transform techniques.

3. Oceanographic data

The site of the lowerings (60°00′N, 29°10′W) is in water approximately 300 m deep on the west side of the main channel of the Denmark Strait. Vertical profiles of temperature, salinity and density (σ_t) were obtained from an independent STD lowering at this location (Fig. 4). A temperature section across the Strait from data collected just prior to the array lowerings together with a general description of the same area from an earlier study (Mann, 1969) indicate that the upper 100 m, represented by $T \approx -1.5$°C and $S \approx 33.5$‰, is part of the East Greenland Current; below is a core of warmer, saltier Atlantic water; and near the bottom is cold water from the western edge of the southward flowing Norwegian Sea Deep Water. Temperature sections show the isotherms to be approximately horizontal for at least 10 km in all directions from our site.

The best indication we have of the amount of internal wave energy present is from a nearby current meter positioned at 300 m depth and 10 km southeast of our site. This mooring had a mean-square velocity of 20 cm^2 s^{-2} for the internal wave band 0.2 cph (cycles per hour) to 2 cph, averaged over the total 32-day record which included our period of observations (C. K. Ross, personal communication). Since a time plot of these current meter data shows approximately the same root-mean-square level throughout the 32-day period, the average is thought to be representative of values at the time of our array observations.

4. Vertical profiles

Vertical profiles of temperature microstructure at a site in the Denmark Strait have structure, spectrum and variance which are similar to those obtained by ourselves and others at various sites near the margins of the oceans. A typical temperature gradient profile obtained from one of the thermometers on one of the lowerings is shown in Fig. 5. Most of the high gradients are concentrated in layers of 10 m or less. While positive and negative gradients are present at all depths, the larger and more numerous gradients are in the direction of the gross change. This bias is expected since integration of the gradient profile gives the temperature profile. Typical values for large gradients are ± 20°C m^{-1}, and peak values reach as high as ± 40°C

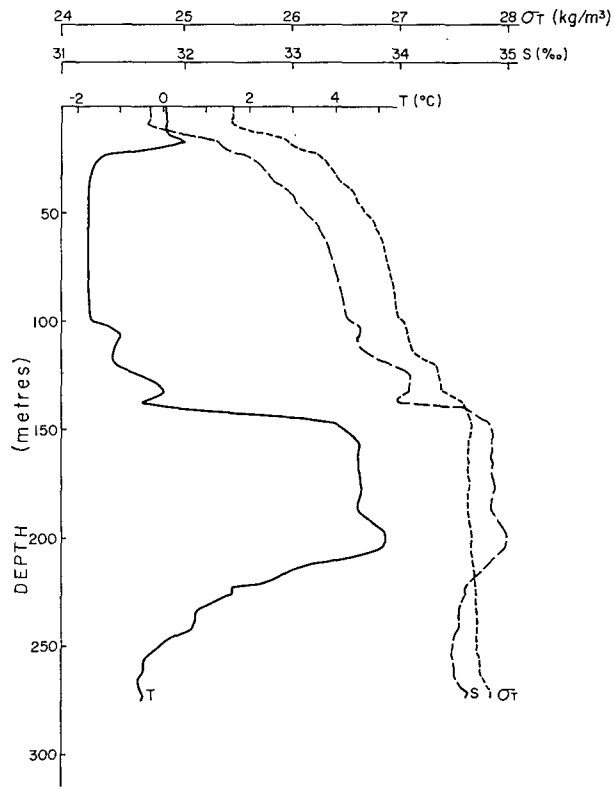

FIG. 4. Vertical profile at the array experimental area obtained with an STD recorder. The figure shows the calculated values of σ_t.

m^{-1}. The ratio of the gradient variance to the square of the mean gradient is high, about 500. On the gross scale the temperature and the salinity are equally important in defining the density. Assuming that the same applies to the small scale, most of the microstructure temperature inversions, i.e., negative temperature gradients, are most likely stable because of a compensating negative salinity gradient.

The array experiment consisted of six lowerings at the same site at approximately 15 min intervals. Two positions of the forward thermometer, T_1, relative to the plane of the other three were used: $D=55$ cm for the first three lowerings and $D=31$ cm for the remaining three.

We have chosen typical examples in Figs. 6a to 6e that illustrate the range of coherence and of tilting of features. The vertical temperature gradient is plotted against depth, with the velocity of the OCTUPROBE being used to convert from a time axis to a depth axis. The time lead of T_1 has been removed in Fig. 6. The sequence T_2-T_1-T_4-T_3 was chosen to partially simulate the geometric arrangement of the probes on the array, counterclockwise when viewed from above. The signal from T_1 appears to have a slightly higher rms level than the other signals. This effect is the result of T_1 having a better response at high frequencies. The gradients are sharper; however, the signal does not contain more structure. We interpret this property to mean that much of the small-scale part of the spectrum of the vertical temperature gradient, smaller than 1 cm, say, is contained in the sharpness of gradients. The lack of an ideal response for the thermometers means an inability to resolve the peak values of a gradient, but we are actually detecting most of the features of the profile. We found that it was easier to trace high gradients among the records than low gradients. Temperature gradient records rather than temperature records have been used for this purpose as they accentuate the microstructure.

In Fig. 6a the four plots of gradient against depth are representative of cases where features are relatively easy to correlate visually. The gradient, or group of gradients marked as A, B, C and D, is continuous between the thermometers. Features near E are not as easy to relate. Frequently a group of gradients such as D is distinctive because of the low gradient above and below rather than the identity of the individual gradients within the group. If a feature such as D is observed at different depths for T_2, T_3 and T_4, we interpret the difference to be a result of a slope to a continuous layer of gradients.

One other commonly observed form of gradient that is easily correlated horizontally is shown in Fig. 6b where the high-gradient region, typically about 20 cm thick, is isolated by layers of relatively uniform temperature water. Individual features such as F and G often occur without large distortion and can thus be related by similarity in the shape of the gradient as well as by position alone. The isolated gradients tend to be low in magnitude and are often found more than a meter from the thick layers of numerous gradients. Occasionally the signature is a double spike, similar to that shown at F and G, indicating a layer of water of relatively uniform temperature between thicker uniform layers. In other cases the shape is more diffuse but rarely with positive and negative gradients together.

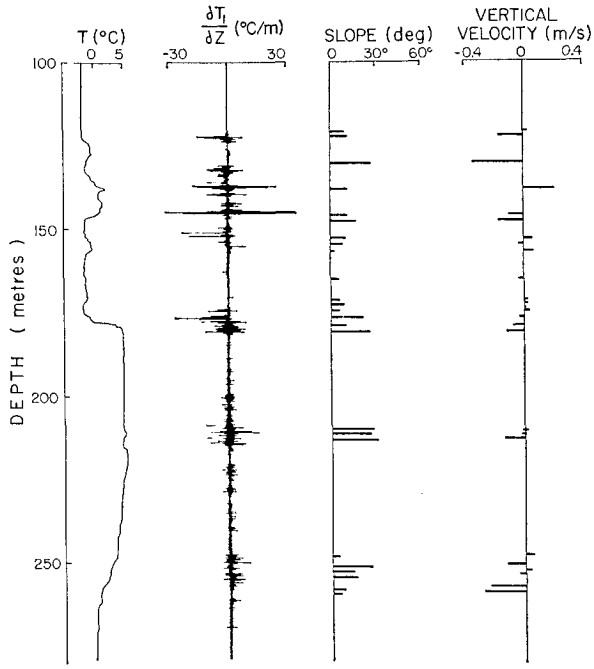

FIG. 5. Vertical profile showing temperature, temperature gradient, and computed slope and vertical velocity of features.

In both of the examples described above the tilt of the features is small; Fig. 6c shows an example of a large tilt. The group of gradients H–J from thermometer T_3 is approximately 30 cm higher than from T_2. For the feature to be continuous between the thermometers it must have a large slope, about 35° between T_2 and T_3 for example. There is also considerable distortion present. The distance H–J in the signal from T_4 is approximately half the thickness measured by T_2 or T_3. Even with this considerable change of thickness the number of gradient spikes remains approximately constant in all samples of H–J. In the signal from T_4 the number of negative gradients is reduced between H–J a region of relative vertical convergence. Instead they appear as low positive gradients—a result of either instrument response being insufficient to resolve them, or horizontal inhomogeneity of the layer. If an internal wave is responsible for this tilt and convergence, the considerable change noted over a distance of 46 cm suggests that the wave is short-crested and of large amplitude.

In many other cases a more pronounced horizontal inhomogeneity made it difficult to identify corresponding features. Fig. 6d is a typical example of such a case.

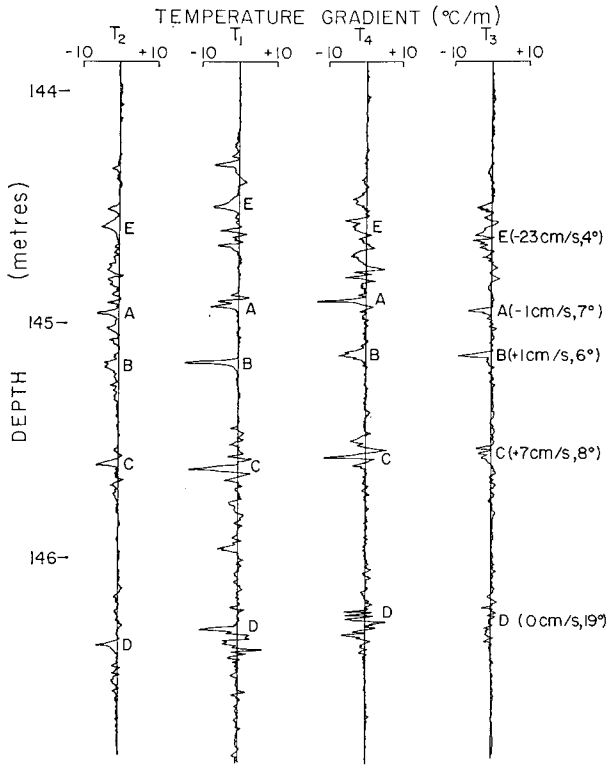

FIG. 6a. Temperature gradients illustrating features easily correlated visually.

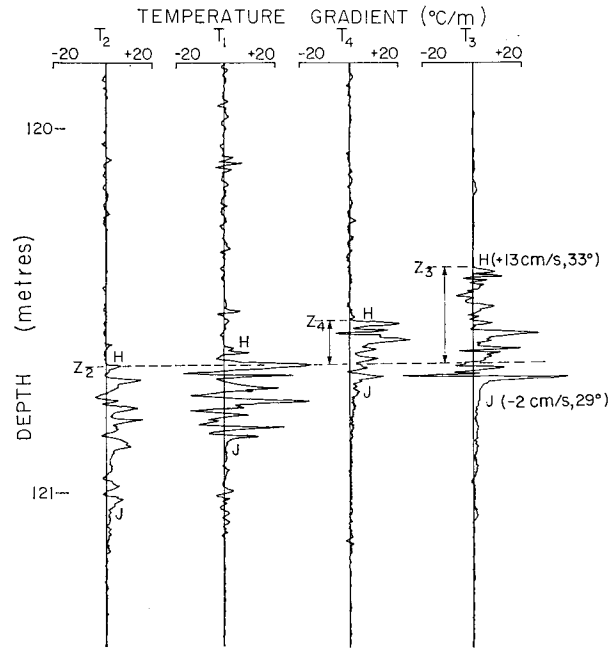

FIG. 6c. Temperature microstructure illustrating large slopes

It is likely that the more energetic ranges K and L are related, however, it is difficult to match them specifically. The inability to visually correlate such a region is not necessarily just a result of greater horizontal in-

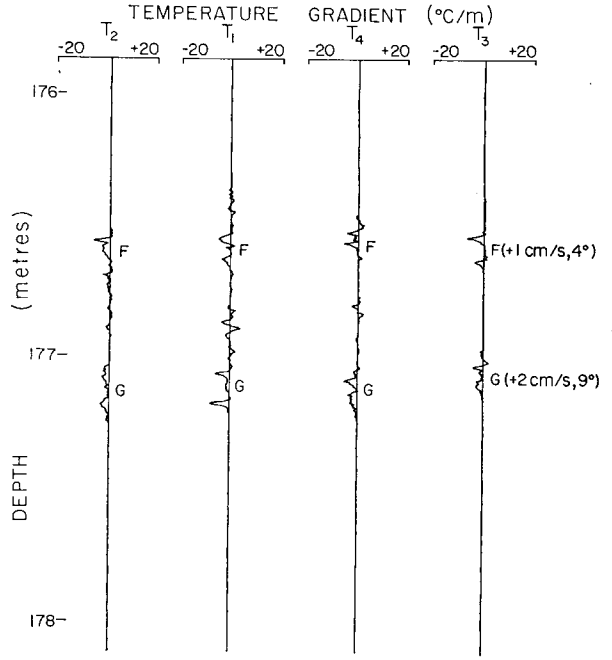

FIG. 6b. High-gradient region about 1 m thick separating two regions of relatively uniform water.

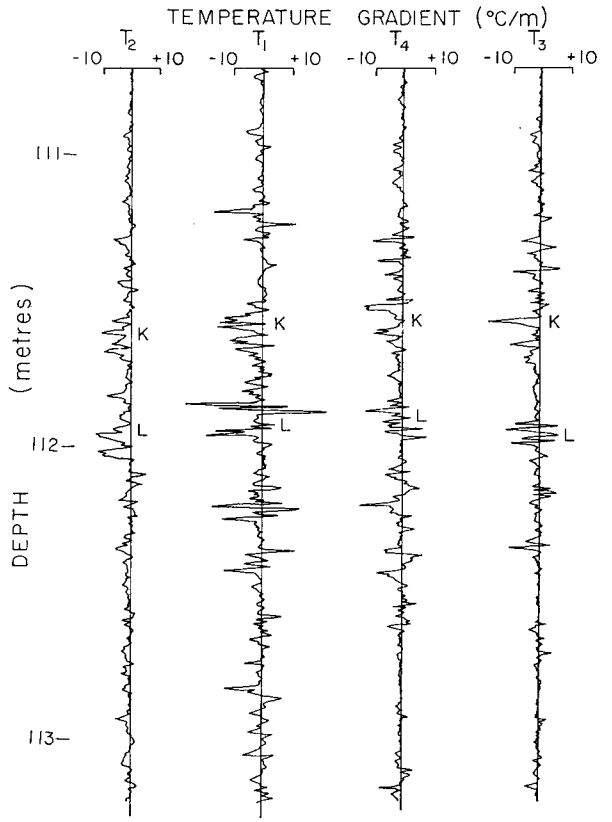

FIG. 6d. Temperature microstructure illustrating pronounced horizontal inhomogeneity.

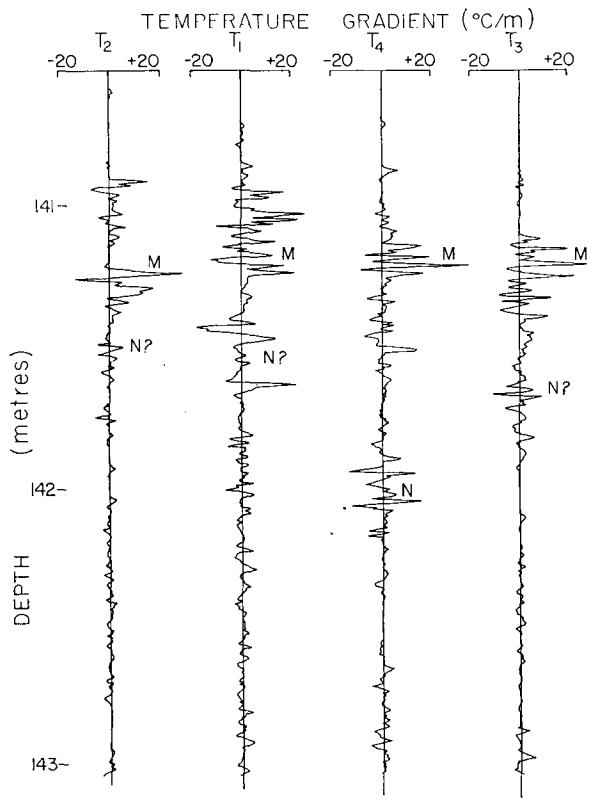

FIG. 6e. Temperature gradient microstructure illustrating possible shear instability.

homogeneity; it is also due to the signal level being relatively constant throughout the layer and there not being a grouping of gradients as illustrated in the previous example. For cases like Fig. 6d, some of the loss of horizontal correlation could be from a tilting and distortion of a group of gradients, likely by short-crested internal waves, and not just from true horizontal inhomogeneity.

One other type of grouping noted in the signals may be related to the formation of the microstructure by shear instability. For cases such as those seen by Woods (1968), the instabilities were often a complete overturning. The instability need not be so violent and may consist entirely of wisps of fluid swept off a wave at the crest. Fig. 6e is an example of the few cases we noted where a group of gradients like M had another energetic group, such as N, adjacent to it but present in the signal of only one or two of the thermometers. We interpret this horizontal inhomogeneity of a large gradient as a possible example of an internal wave breaking, layer N being water out of the layer M. The vertical scale of the phenomena is typically less than 1 m.

5. Time dependence and slope

The gradient records were examined to find cases where it was possible to correlate visually the same feature in the four signals. Assuming that the gradient was horizontally continuous, the relative depth of the gradient from each thermometer was used to calculate a time dependence and a slope. In order to have estimates of time dependence and slope spread throughout the record, one feature per meter was chosen as representative of the features within that meter. After some experience with the data we felt that the relative depth of an identifiable feature such as the maximum of a gradient could be determined to ± 2 cm. The sampling method is biased to those cases where features could be visually correlated (which includes three-quarters of the high-gradient data sections).

The display (Fig. 6) of the signals from the three thermometers T_2-T_1-T_4 contains a time dependence because thermometer T_1 leads the other thermometers. Since the three thermometers were equi-spaced horizontally, a feature with no curvature or vertical velocity will be observed by T_1 at a depth midway between the depths at which it is observed by T_2 and T_4; this was not the usual case. Therefore, there existed curvature, vertical velocity or both. We do not have data where the distance D that T_1 is ahead of the other thermometers is zero, and are thus unable to estimate curvature alone. Instead, we use the distance Δz_c between the observation of a feature in T_1 and the point midway between the same feature in T_2 and T_4 as a measure of curvature. If, on the other hand, the curvature were zero and the shift due to a local vertical velocity W, this velocity would have a magnitude

$$W=\frac{D-V\Delta t}{\Delta t}=\frac{\Delta z_c}{\Delta t}. \tag{1}$$

The vertical velocity and Δz_c are chosen positive upward, V is the velocity of OCTUPROBE, and Δt the time interval between the feature being observed at thermometer T_1 and the average time observed at thermometers T_2 and T_4. The accuracy of estimating Δz_c and W is about ± 4 cm and ± 6 cm s^{-1}, respectively; it depends upon the ability to position a particular feature (about ± 2 cm or ± 0.02 s) and the uncertainty in the probe velocity (± 5 cm s^{-1}).

The other parameter calculated using the temperature gradient plots is the slope of a feature. When a feature is observed at different depths by the three thermometers T_2, T_3 and T_4, it must be inclined to the horizontal. As a measure of this slope we calculated the angle θ between the vertical and the normal to the plane defined by the particular feature. The formula is

$$\left.\begin{aligned}\cos\theta=\sin\zeta[&\tan^2\alpha+\tan^2\beta\\&-2\cos\gamma\tan\alpha\tan\beta+\sin^2\zeta]^{-\frac{1}{2}}\\ \tan\alpha=\frac{z_2-z_4}{R},\quad &\tan\beta=\frac{z_2-z_3}{R}\end{aligned}\right\}. \tag{2}$$

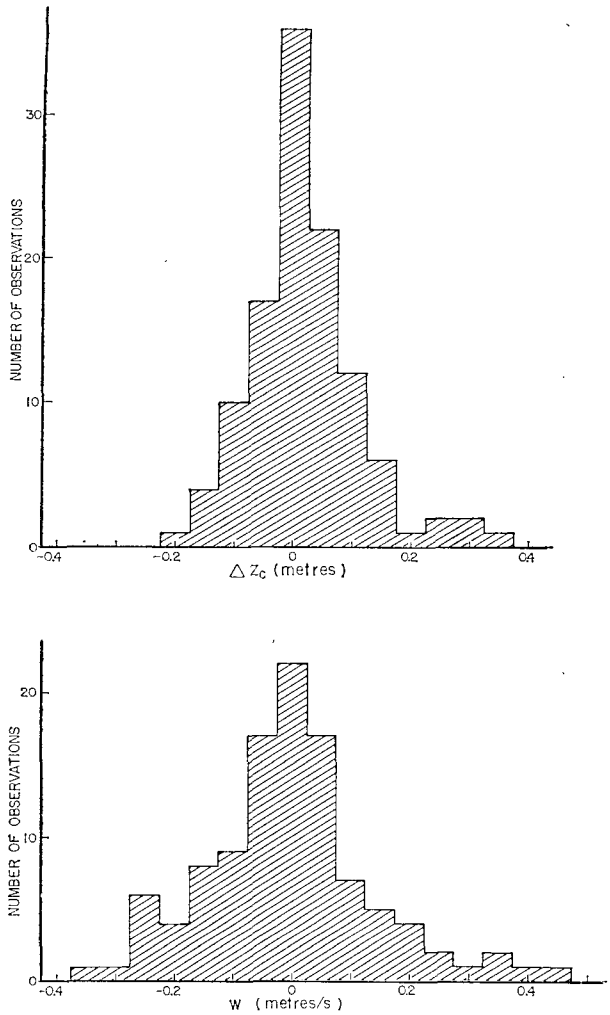

FIG. 7. Distribution of vertical velocity W calculated from microstructure gradients assuming no curvature and curvature Δz_c calculated assuming no vertical velocity.

If z_2, z_3 and z_4 are the positions of the particular feature in T_2, T_3 and T_4, as illustrated in Fig. 6c, then α and β are the angles between the horizontal and the lines z_2z_3 and z_2z_4 and ζ is the angle between the projection of z_2z_3 and z_2z_4 on the horizontal, equal to 60° for the array data. R is the horizontal separation of the sensors. Because of the error in estimating the appropriate depth of a feature and the tilt of OCTUPROBE ($\pm 2°$ to $\pm 3°$ maximum), the accuracy for the angle θ is about $\pm 5°$.

For each of the lowerings it was possible to find approximately 25 cases where tilt and velocity could be calculated. Typical results are shown in Fig. 5. The upper 100 m, water of the East Greenland Current, was fairly uniform in temperature and not used in these calculations. Since the high gradients tend to be concentrated in layers of order 1 m to 10 m thick, the estimate of slope and velocity is also limited to these layers. As a result the vertical sequence is typically a few points approximately 1 m apart, broken by large gaps. Even so, many examples show large changes in slope and vertical velocity between estimates separated by just 1 or 2 m. If the slope and velocity are entirely due to a wave motion within the water column, some of the waves present must have a small vertical scale, of order 1 m. A possible explanation that could account for the short vertical and horizontal wavelengths and high tilt is that shear instability waves, possibly generated by larger scale internal waves, are present.

We have no direct evidence that the vertical velocity (or curvature) of a given feature has zero average or that the slope of a gradient actually oscillates about a mean (horizontal) position, such as would be expected if the variation of these parameters is a result of internal waves. Similar statistics can be inferred by assuming that all the data collected by spatial sampling will have the same averages and distributions as a time series of one feature.

The distribution of the vertical velocity and slope and the phase between the two are consistent with a model of an internal wave field with a Gaussian amplitude distribution passing through horizontally layered microstructure.

For a random wave field a histogram of the vertical velocity W and the curvature measure Δz_c would have zero mean and Gaussian shape. The array data are shown in Fig. 7. W and Δz_c were evaluated assuming that the other was negligible. These magnitudes are similar to those expected from internal waves. Root-mean-square values for W and Δz_c are ± 10 cm s^{-1} and ± 5 cm, respectively. A current meter located in the vicinity of the site measured internal wave velocities

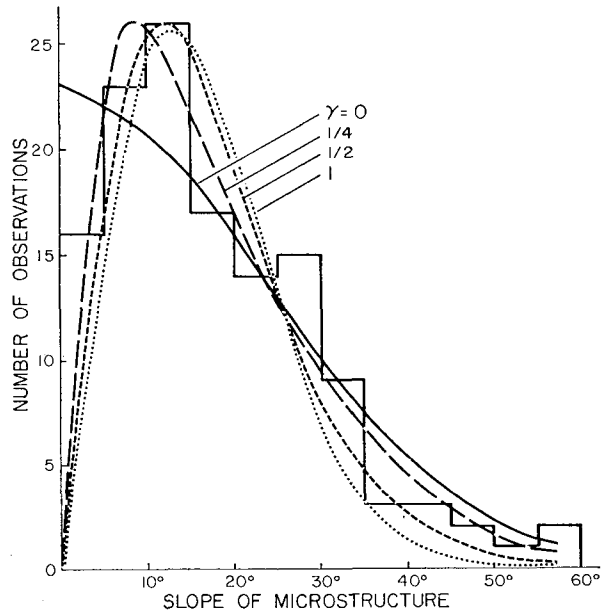

FIG. 8. Distribution of slope of microstructure from all array lowerings.

of ± 5 cm s^{-1}, a value slightly lower than those calculated from the array data. The current meter data are limited to frequencies lower than 2 cph and do not include high-frequency waves of the type associated with shear instabilities. The rms value for Δz_c implies short-crested waves. We feel that vertical velocity and curvature are both important in explaining the data.

The distribution of the tilt angles, or slopes, for the microstructure is plotted in Fig. 8. An rms value of about 25° and angles as high as 40° to 60° suggest that many of the tilts must be from short-crested waves. The shape of the histogram for tilt is compared with the theoretical distribution predicted by Longuet-Higgins (1957) for the slope of a sea surface subjected to waves with Gaussian amplitude distribution. Although the theoretical calculations are for the sea surface, the results as they pertain to wave slopes apply to an internal wave field. The parameter γ is a measure of the long-crestedness of the waves or alternately the range of directions from which the waves are propagating. Waves from a single direction, $\gamma=0$, will have a Gaussian distribution for the slope; a wave field with equal energy from all directions, $\gamma=1$, has a Rayleigh distribution. Some intermediate value for γ, about $\frac{1}{4}$, gives the best least-squares fit, as suggested from Fig. 8.

For a random wave field the slope and vertical velocity (or curvature) should be uncorrelated and, as shown in Fig. 9 for the array data, these values bear no strong relationship.

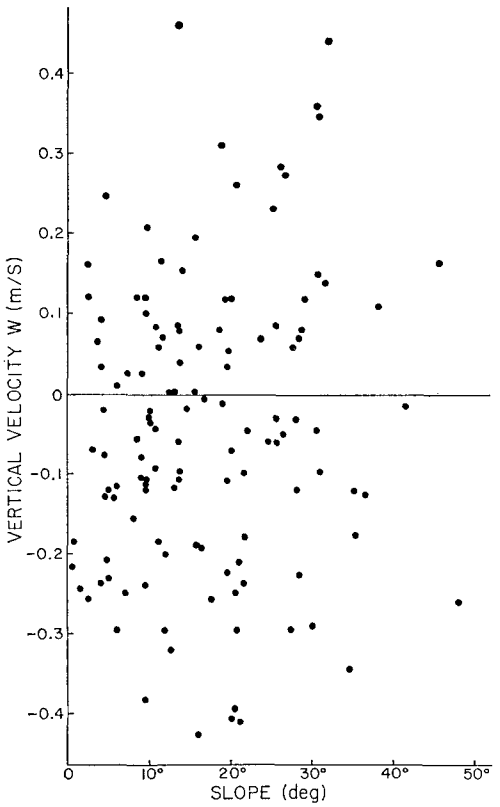

FIG. 9. Scatter diagram relating vertical velocity and slope of temperature microstructure.

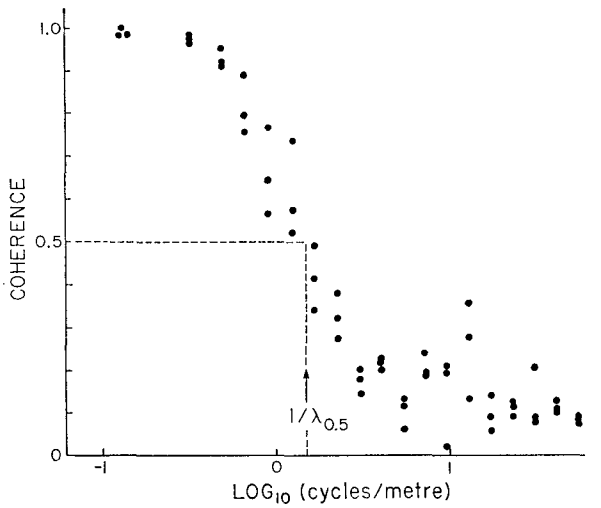

FIG. 10. Average coherence spectra between pairs of thermometers in array plane (T_2,T_3,T_4) for one lowering.

It is interesting to note that if the large tilting of microstructure is typical for the oceans, horizontal tows through these layered features would create the false impression of a structure more isotropic than it really is.

6. Horizontal correlation

For each pair of thermometers in the array we computed the coherence between the gradient signals, averaged over a total depth of $\sim$200 m. Coherence is the square root of the normalized cospectrum and quadspectrum. The signal from thermometer T_1 was shifted to compensate for the vertical separation. Typical coherence spectra (Fig. 10) show that large-scale features with vertical wavelengths >1 m are highly coherent, while those at smaller scales, less than 20 cm, are incoherent. The fall-off between the high-coherence scales and the low-coherence scales occurs in less than a decade of wavelength and corresponds to the spectral division between intermediate scale and microstructure. Thus, when averaged over the 200 m, two simultaneous vertical profiles with 46 cm separation have coherent intermediate scales and incoherent microstructure.

For the purpose of comparison of the data obtained from different profiles and different separations of sensors, we define the wavelength $\lambda_{0.5}$, at which the coherence drops to 0.5, as representative of the division between high- and low-coherence scales. The value of $\lambda_{0.5}$ is shown in Fig. 11 plotted as a function of the horizontal separation of sensors. Included in the plot along with the array data are values for 5 cm separation taken from lowerings at a station $\sim$20 km southeast of the array site, examples with 41 cm separation from

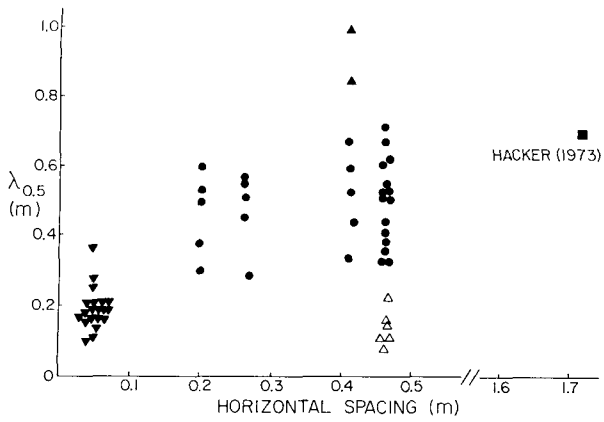

FIG. 11. Summary of $\lambda_{0.5}$ for various spacings of thermometers: ▼, Denmark Strait; ● and △, array data; ▲, Gulf Stream; ■, San Diego Trough (Hacker, 1973). Solid symbols show averages over 200 m depth, open symbols over 5 m.

data collected in the vicinity of the Gulf Stream, and one value from Hacker (1973). For all these cases the averaging depth is again approximately 200 m. As expected, the signals from sensors with 5 cm separation were coherent to smaller scales. For separations $\gtrsim 25$ cm, $\lambda_{0.5}$ has already approached the wavelength which approximately divides the larger intermediate scale irregularities and the smaller scale microstructure; that is, the intermediate scales are coherent, the microstructure incoherent.

We know, however, as shown in Fig. 6, that it is possible to correlate visually among the array sensors, even in detail, a larger number of gradients with a vertical scale $\lesssim 10$ cm. The reason that this visual correlation is not reflected by the coherence spectrum is that most of these samples exhibit a relative vertical displacement or a distortion or both, properties that can be interpreted to be the result of an internal wave. Such internal waves and their associated shears will appear as an increase in the horizontal inhomogeneity. For the array data, the rms tilt of 25° represents a vertical shift of about 20 cm for a point 46 cm away. Since there is little correlation between gradients with a 20 cm vertical separation, a random shift of this magnitude is sufficient to produce a corresponding low horizontal correlation at scales of about 10 cm.

To obtain an estimate of a representative $\lambda_{0.5}$ wavelength for the microstructure in the absence of tilt or distortion by an internal wave, we computed the coherence spectrum for a 5 m depth range from one of the lowerings where the slope and vertical velocity happened to be small and nearly constant. This same patch of microstructure had larger slopes in other lowerings. The plot of the coherence spectrum for the 5 m sample has considerably more scatter than those obtained from the 200 m averages; the values of $\lambda_{0.5}$ were taken from the mean curve drawn among the points. When plotted in Fig. 11 (open symbols) the $\lambda_{0.5}$ are seen to be much smaller than values from the same lowering that have been averaged over a larger depth interval. We consider the smaller values of $\lambda_{0.5}$, about 10 cm, to be typical for the microstructure at this site, after allowing for tilting. The actual thickness of a feature is approximately half of $\lambda_{0.5}$. Features of vertical thickness 5 cm and larger are coherent for the 46 cm separation of the array. Thus for the array data, microstructure with vertical scales of order 5 cm or larger have a horizontal to vertical scale ratio of at least 10 to 1. This ratio is consistent with visual correlation between the signals.

7. Summary

The three-dimensional organization of microstructure features has been examined using a four-thermometer array in Denmark Strait. The profiles of vertical temperature gradient show many patches of irregular high gradients, each composed of detailed features at scales of 10 cm or less. The spectrum of these gradients peaks at a scale of a few centimeters and the ratio of temperature variance to the mean square temperature gradient is about 500.

Most features of a vertical scale greater than about 10 cm could be identified in all four temperature signals by the similarity in shape. Therefore these structures are in the form of "layers" of at least 46 cm in horizontal extent having temperature gradients along the layers which are much smaller than the corresponding vertical temperature gradients. These layers were not always horizontal. Individual features were found to have slope and vertical velocity or curvature, properties that can be interpreted to be the result of an internal wave field superimposed upon layered microstructure. The high rms tilt of 25°, significant divergence or convergence over the dimensions of the array, and lack of a strong coherence vertically for the slope and vertical velocity suggest that many of the waves distorting the microstructure are high-amplitude, short-crested waves. These waves may be the mechanism for generating the microstructure.

For a 5 m section of a lowering where features were mostly horizontal, the signals from sensors spaced 46 cm apart had a coherence greater than 0.5 for features with a vertical thickness greater than 5 cm. Thus at the Denmark Strait site features with a vertical thickness of about 5–10 cm have a horizontal scale of at least an order of magnitude larger than the vertical scale. To maintain such layers as a stable configuration, buoyancy forces must play a significant role in the dynamics of the microstructure, at least down to scales of about 5 cm thickness. Gregg *et al.* (1973) estimate the viscous and diffusive cutoff for typical oceanic cases to be about 1 cm. If the smallest scale dominated by buoyancy forces is of the same order as the largest scale with significant diffusive and viscous action, it is unlikely that the life history of most oceanic microstruc-

ture, from generation to dissipation, is sufficiently energetic that the properties of isotropic turbulence can be used to describe or evaluate rates of transfer or levels of dissipation.

REFERENCES

Fabula, A. G., 1962: The plume test method of determining the dynamic response of towed thermometers. Rept. 62–3, Defence Research Establishment, Pacific, Victoria, B. C.

Garrett, C., and W. Munk, 1972: Oceanic mixing by breaking internal waves. *Deep Sea Res.*, **19**, 823–832.

Gregg, M. C., C. S. Cox and P. W. Hacker, 1973: Vertical microstructure measurements in the central North Pacific. *J. Phys. Oceanogr.*, **3**, 458–469.

Hacker, P. W., 1973: The mixing of heat deduced from temperature fine structure measurements in the Pacific Ocean and Lake Tahoe. Ph.D. thesis, University of California, San Diego.

Longuet-Higgins, M. S., 1957: The statistical analysis of a random, moving surface. *Phil. Trans. Roy. Soc. London*, **A249**, 321–387.

Mann, C. R., 1969: Temperature and salinity characteristics of the Denmark Strait overflow. *Deep Sea Res.*, **16**, Suppl., 125–137.

Osborn, T. R., and C. S. Cox, 1972: Oceanic finestructure. *Geophys. Fluid Dyn.*, **3**, 321–345.

Stommel, H., and K. N. Federov, 1967: Small-scale structure in temperature and salinity near Timor and Mindanao. *Tellus*, **19**, 306–325.

Woods, J. W., 1968: Wave-induced shear instability in the summer thermocline. *J. Fluid Mech.*, **32**, 791–800.